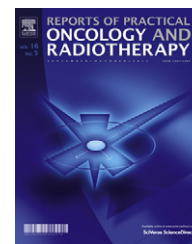


Available online at www.sciencedirect.com

SciVerse ScienceDirect

journal homepage: <http://www.elsevier.com/locate/rpor>

Original article

Effect of the bone heterogeneity on the dose prescription in orthovoltage radiotherapy: A Monte Carlo study

James C.L. Chow^{a,b,*}, Grigor N. Grigorov^c^a Radiation Medicine Program, Princess Margaret Hospital and Department of Radiation Oncology, University of Toronto, Toronto, ON M5G 2M9, Canada^b Department of Physics, Ryerson University, Toronto, ON M5B 2K3, Canada^c Department of Medical Physics, Grand River Regional Cancer Center, Kitchener, ON N2G 1G3, Canada

ARTICLE INFO

Article history:

Received 3 June 2011

Received in revised form

5 August 2011

Accepted 25 September 2011

Keywords:

Orthovoltage photon beam

Orthovoltage radiation therapy

Monte Carlo simulation

Bone backscatter and surface dose

ABSTRACT

Background: In orthovoltage radiotherapy, since the dose prescription at the patient's surface is based on the absolute dose calibration using water phantom, deviation of delivered dose is found as the heterogeneity such as bone present under the patient's surface.

Aim: This study investigated the dosimetric impact due to the bone heterogeneity on the surface dose in orthovoltage radiotherapy.

Materials and methods: A 220 kVp photon beam with field size of 5 cm diameter, produced by a Gulmay D3225 orthovoltage X-ray machine was modeled by the BEAMnrc. Phantom containing water (thickness = 1–5 mm) on top of a bone (thickness = 1 cm) was irradiated by the 220 kVp photon beam. Percentage depth dose (PDD), surface dose and photon energy spectrum were determined using Monte Carlo simulations (the BEAMnrc code).

Results: PDD results showed that the maximum bone dose was about 210% higher than the surface dose in the phantoms with different thicknesses of water. Surface dose was found to be increased in the range of 2.5–3.7%, when the distance between the phantom surface and bone was increased in the range of 1–5 mm. The increase of surface dose was found not to follow the increase of water thickness, and the maximum increase of surface dose was found at the thickness of water equal to 3 mm.

Conclusions: For the accepted total orthovoltage radiation treatment uncertainty of 5%, a neglected consideration of the bone heterogeneity during the dose prescription in the sites of forehead, chest wall and kneecap with soft tissue thickness = 1–5 mm would cause more than two times of the bone dose, and contribute an uncertainty of about 2.5–3.7% to the total uncertainty in the dose delivery.

© 2011 Greater Poland Cancer Centre, Poland. Published by Elsevier Urban & Partner Sp. z.o.o. All rights reserved.

* Corresponding author at: Radiation Medicine Program, Princess Margaret Hospital and Department of Radiation Oncology, University of Toronto, Toronto, ON M5G 2M9, Canada. Tel.: +1 416 946 4501x5089; fax: +1 416 946 6566.

E-mail address: james.chow@mp.uhn.on.ca (J.C.L. Chow).

1507-1367/\$ – see front matter © 2011 Greater Poland Cancer Centre, Poland. Published by Elsevier Urban & Partner Sp. z.o.o. All rights reserved.
doi:10.1016/j.rpor.2011.09.001

1. Background

Orthovoltage radiotherapy has a long history of over 60 years of treatment of superficial tumors such as basal cell carcinoma, squamous cell carcinoma and melanoma.^{1–3} In some skin treatment sites, such as the forehead, chest wall, skin over the cheekbone and kneecap, soft tissue of thickness equal to about 1–5 mm is over the bone of skull, rib or patella, respectively. When skin tumor in the above sites is irradiated by orthovoltage photon beams, the presence of bone heterogeneity affects the surface dose in the treatment due to the changed backscatter contribution, as water is replaced by the bone. Since bone heterogeneity is not considered in dose calculation based on dose calibration using a water phantom, an underestimation of dose might occur when it is prescribed. This effect of surface dose enhancement due to bone backscatter is more significant in the high orthovoltage photon energy of 220 kVp than the lower superficial photon energies such as that of 100 kVp.⁴

2. Aim

To investigate the impact of the surface dose variation due to the presence of bone heterogeneity, a photon energy spectral study was carried out using a heterogeneous phantom and Monte Carlo simulation. The photon energy spectra at the phantom surface were determined with different thicknesses of water. These energy spectra of photons and backscattered photons helped us to understand in detail the relationship between the surface dose variation and thickness of the overlaying tissue. A Gulmay D3225 orthovoltage X-ray machine (Gulmay Medical Ltd., UK) which produces a photon beam with energy of 220 kVp was modeled for Monte Carlo simulations using the BEAMnrc code to study this problem. The aim of this study was to investigate the impact of dosimetric uncertainty when bone heterogeneity is present and underneath the patient's surface of soft tissue (millimeter scale), as prescribed dose calculation is based on absolute dose calibration using a homogeneous (water) phantom.

3. Materials and methods

3.1. Phantom and calculated geometry

A heterogeneous phantom containing water (thickness = 1–5 mm) over the bone (thickness = 1 cm) was used as shown in Fig. 1. The phantom was irradiated by an orthovoltage photon beam perpendicular to the phantom surface. The energy of the beam and source-to-surface distance (SSD) were equal to 220 kVp and 20 cm, respectively. A treatment cone with diameter equal to 5 cm was used to conform the beam field. This treatment cone was examined in this study because it was typical and generally used as a reference cone for the backscatter and relative exposure factor. Percentage depth dose (PDD) was calculated along the central beam axis (vertical broken line) in the phantom. The photon energy spectra were determined based on the particle scoring planes at the phantom surface. For the purpose of dosimetry

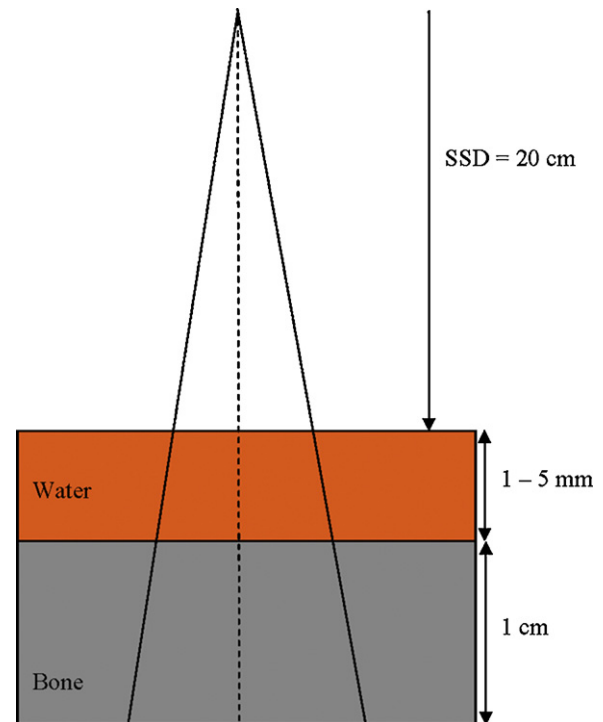


Fig. 1 – Schematic diagram (not to scale) showing the calculation geometry of the surface dose and PDD for different thicknesses (1–5 mm) of water on top of the bone. The thickness of bone is 1 cm.

comparison and determining the relative results, all Monte Carlo simulations were repeated in a water phantom using the same calculated geometry with the bone layer replaced by water.

3.2. Monte Carlo simulation

The Electron Gamma Shower (EGSnrc) code (version 4-r2-2-4) developed by the National Research Council of Canada was used.⁵ In this code, the shape of the X-ray energy spectra is improved by implementing the electron impact ionization model.⁶ Moreover, the efficiency of energy transition from the electron current to photons is increased by including a directional bremsstrahlung splitting.⁷

3.2.1. Monte Carlo modeling and verification of the orthovoltage photon beam

A 220 kVp photon beam produced by a Gulmay D3225 orthovoltage X-ray machine was used in this study. An open circular end fixed applicator with diameter of 5 cm and SSD = 20 cm was used. The BEAMnrc⁸ was used to generate a phase-space file based on the treatment head data of geometries and materials of different components such as the X-ray tube, primary collimator, filter, ionization chamber and applicator, provided by the manufacturer and Knoos et al.⁹ In our 220 kVp photon beam, 1.2 mm of Cu and 1 mm of Al were used as a filter to define the beam quality. The energy cut off for electron and photon transport was set at 521 keV and 1 keV, respectively. A phase-space file including information of the energy,

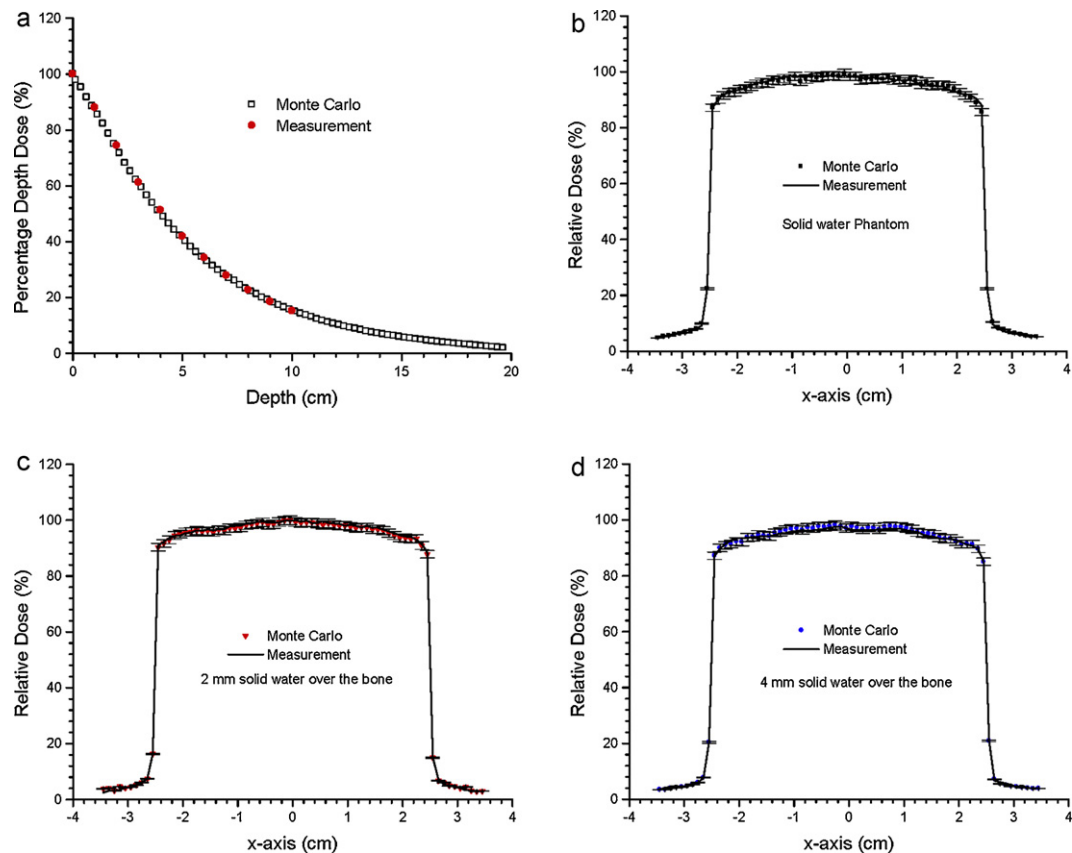


Fig. 2 – (a) PDDs of a 220 kVp photon beam with circular field of diameter = 5 cm and SSD = 20 cm in water. The depth doses were calculated and measured using Monte Carlo simulation and parallel-plate ionization chamber, respectively. Beam profiles of the 220 kVp beam at the phantom surface for a (b) solid water phantom, (c) 2 mm of solid water over the bone and (d) 4 mm of solid water over the bone, calculated and measured using Monte Carlo simulation and Gafchromic EBT film. All doses in the beam profiles are normalized to the maximum dose. The error bars in (b–d) represent uncertainty of $\pm 1\%$.

orientation, type, charge and position of particles crossing the scoring plane at the bottom of the applicator was generated containing about 36 million particles.

Verification of the phase-space beam was carried out by comparing the PDD calculated and measured by Monte Carlo simulation and parallel-plate ionization chamber (PS-033, Capintec Inc., New Jersey) using the solid water phantom (30 cm \times 30 cm \times 10 cm), as shown in Fig. 2(a). The same experimental configurations of the beam and phantom geometry were used for Monte Carlo simulation with the voxel size set at 0.25 cm \times 0.25 cm \times 0.25 cm. It can be seen that the PDD results of Monte Carlo simulation and measurement agreed well within a deviation of $\pm 1\%$ at 1 sigma. In addition, the surface beam profiles for a solid water phantom (Fig. 2(b)), heterogeneous phantoms with 2 (Fig. 2(c)) and 4 mm (Fig. 2(d)) of solid water over a bone slab of 1 cm (GAMMEX model: 450-220, Middleton, WI) calculated by Monte Carlo simulations were compared to measurements using Gafchromic EBT films. Again, both Monte Carlo and measured results agreed well within a deviation of $\pm 1\%$. Verification of the peak scattering factor was also carried out by comparing the Monte Carlo results with those according to the AAPM TG-61.¹⁰ The Monte Carlo model of the 220 kVp photon beam was therefore validated.

3.2.2. Dose calculation of phantoms using the DOSXYZnrc

The surface doses and PDDs of the phantom in Fig. 1 were calculated using the DOSXYZnrc.^{11,12} The voxel size used in the simulation was 0.1 mm \times 0.1 mm \times 0.1 mm, which corresponds to the x, y and z-axis. Under this calculation set up, the surface dose in this study was defined at the depth of 0.05 mm. This is the average energy deposited in the center of the first voxel in the phantom. One hundred and fifty million histories were run in each calculation as per thicknesses of water equal to 1, 2, 3, 4 and 5 mm in the phantom of Fig. 1. In the simulation, PRESTA II was selected for the electron-step algorithm.¹³ The spin effect, bound Compton scattering, Rayleigh scattering, atomic relaxation and electron impact ionization were all set at ON. The energy cut off for electron and photon transport was equal to 521 keV and 1 keV in the simulation, respectively. Under this approach, the relative dose error (statistical uncertainty as a fraction of dose in the voxel) for the surface voxel was found to be around 0.5% at 1 sigma based on the Monte Carlo results using the same number of histories.^{11,14} In this study, ICRPBONE700ICRU with mass density of bone equal to 1.85 g cm⁻³ was selected as bone material in the simulations. The surface doses and PDDs of the heterogeneous (Fig. 1) and homogeneous (bone replaced with water) phantoms were calculated.

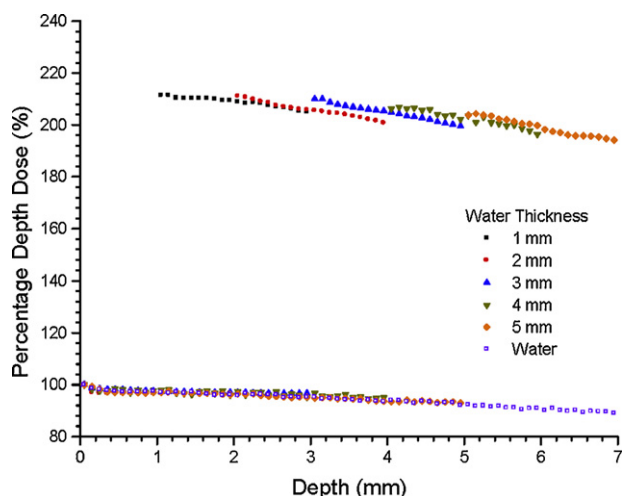


Fig. 3 – PDDs of the 220 kVp photon beam in phantom as shown in Fig. 1 with thicknesses of water equal to 1–5 mm, calculated by Monte Carlo simulations. PDD of the water phantom with the same calculation configuration is also shown in the figure for comparison. Doses in the PDD curve are all normalized to the surface of the corresponding phantom with specific thickness of water over the bone.

3.2.3. Calculation of energy spectrum using the BEAMnrc and BEAMDP

The photon fluence at the phantom surface was determined from the phase spaces which included the multiple crossers (backscattered photons) calculated by the BEAMnrc. The BEAMDP⁸ was used to calculate the energy spectrum based on the photon fluence. The number of bins in the photon energy spectrum was set at 200 in the range of 0–250 keV. Photon energy spectra at the phantom surface were determined with thicknesses of water equal to 1–5 mm. The SSD was kept constant (20 cm) when the thickness of water was changed in the phantom. In comparison, Monte Carlo simulations were repeated in pure water phantoms with the same calculation configurations of the heterogeneous phantoms.

4. Results

The PDDs of the 220 kVp photon beams (field size = 5 cm diameter; SSD = 20 cm) for the heterogeneous phantom in Fig. 1 are shown in Fig. 3 with thicknesses of water equal to 1–5 mm. The PDD of the water phantom (i.e. bone replaced with water) is also shown in Fig. 3 for comparison. All doses in Fig. 3 are normalized at the phantom surface to illustrate the dose enhancement in the bone layer. Fig. 4 shows the relative surface dose (surface dose of phantom with bone to without bone) varying with the thickness of water over the bone. The surface doses in Fig. 4 are therefore normalized to the surface dose of a water phantom (relative dose = 100%) with the same dimension by considering the surface voxels at the same position of the heterogeneous and water phantom. Fig. 5 shows the photon energy spectra at the phantom surface with different thicknesses of water equal to 1, 3 and 5 mm over the bone. Photon energy spectrum at the surface of a pure water phantom

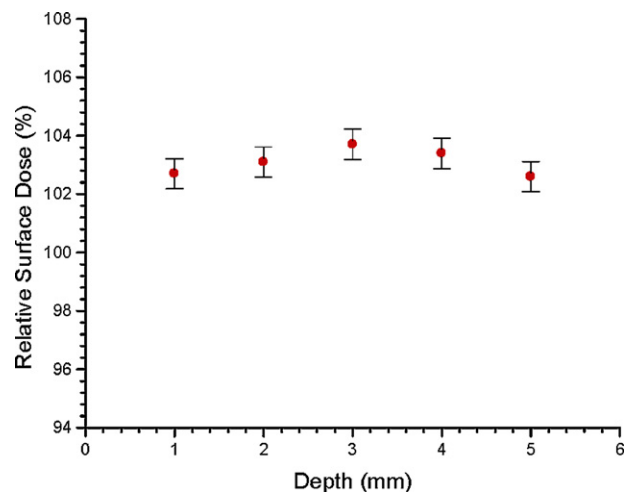


Fig. 4 – Relative surface dose (surface dose ratio in percentage with to without a bone) varying with the thickness of water over the bone. Doses are normalized to the surface dose of a water phantom with the bone (Fig. 1) replaced with water. The error bar represents $\pm 0.5\%$.

is also included in Fig. 5 for comparison. Spectral curves in Fig. 5 are all normalized to the total areas of the curves.

5. Discussion

5.1. PDDs and surface doses of the phantoms

Fig. 3 shows the PDDs of the phantoms in Fig. 1 with different thicknesses of water, and all depth doses in the curve are normalized to the surface of corresponding phantom with specific thickness of water. Under this approach, the bone dose enhancement can be seen clearly compared to the surface dose. Comparing PDDs of the water phantom with that of the bone in the phantom replaced with water, it can be seen in

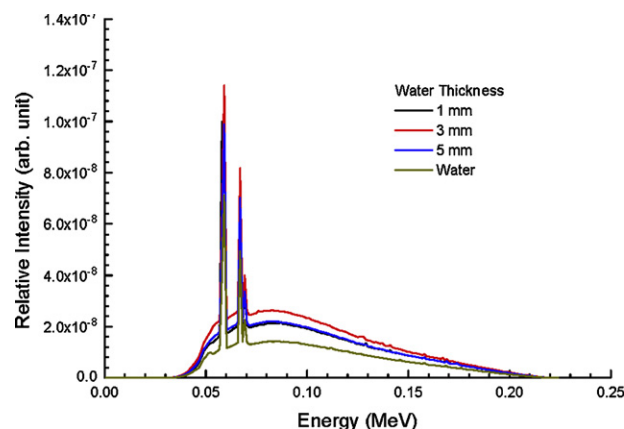


Fig. 5 – Relative photon energy spectra at the phantom surface varying with the thicknesses of water equal to 1, 3 and 5 mm. Photon energy spectrum at the same position of the phantom surface using a pure water phantom is included for comparison. All spectral curves are normalized to the total area of the corresponding curves.

Fig. 3 that the maximum increase of dose is about 210% in the bone. This bone dose enhancement can be explained as the increase of the interaction cross-section for the photoelectric effect with a high atomic number and photon beam energy in the kV range.^{15,16} The variation of bone doses is between 205% and 211% for the thickness of water ranging from 1 to 5 mm, and it shows that the dependence of water thickness on the bone dose is insignificant under such range. Although the increased bone dose would increase the patient's complication rate to the red bone marrow and bone surface cells as radiosensitive organs at risk, it should be noted that this study is not focused on the bone dose enhancement as it is a well-known phenomenon. Instead, our study makes emphasis in the dosimetric impact on the surface dose due to the presence of bone heterogeneity, and the relative surface dose varying with the thickness of water can be seen in Fig. 4. In Fig. 4, all surface doses of bone phantoms are normalized to the surface dose of a water phantom. With this normalization approach, the increase of surface dose due to the presence of the bone can be seen. Moreover, the relative surface doses in Fig. 4 represent the variation of prescribed dose at the patient's surface, when the surface dose is affected by bone heterogeneity as per the phantom geometry in Fig. 1. It is seen in Fig. 4 that the surface dose is increased between 2.5% and 3.7% when the thickness of water is increased in the range of 1–5 mm over the bone. In orthovoltage radiotherapy, since the dose prescription at the patient's surface is done by assuming the patient's body is homogeneous according to the absolute dose calibration, an underestimation of 2–4% of a prescribed dose might occur. This dosimetric uncertainty will narrow down the total treatment uncertainty of 5% including the uncertainties of patient setup, dose calibration and dose calculation.^{17,18}

5.2. Photon fluence spectral analyses

Fig. 5 shows the photon energy spectra at the phantom surface for thicknesses of water equal to 1, 3 and 5 mm. The spectral curves in Fig. 5 are normalized to the total area of the curve, and it is seen clearly that the relative intensities of the photon spectra using the heterogeneous phantom are higher than that of the spectral curve using a pure water phantom. Moreover, a relative intensity of the spectral curve for water thickness of 3 mm is higher than those of 1 and 5 mm. This gives the maximum surface dose at thickness of water equal to 3 mm, while surface doses of 1 and 5 mm of water are close, as shown in Fig. 4. The surface dose is affected by bone heterogeneity due to two effects: the loss of backscatter compared to the full scattering condition and bone backscatter to the phantom surface.^{16,19} The effect of loss of backscatter decreases the surface dose while the effect of bone backscatter increases the dose. Since both effects become weaker with the bone located further from the phantom surface, the combination of these two effects results in a maximum surface dose at the bone depth of 3 mm in this study.

6. Conclusion

In orthovoltage radiotherapy of soft tissue over the bone, the dosimetric impact when the treatment dose is prescribed at

the patient's surface was investigated by a clinical orthovoltage photon beam using Monte Carlo simulation. Results based on the treatment cone of 5 cm in diameter showed that an increase of the surface dose of 2.5–3.7% was found when the distance between the phantom surface and the bone was increased to the range of 1–5 mm. This increased surface dose results in additional dosimetric uncertainty that narrows down the total error margin (5%) concerning the patient setup and machine calibration in a clinical dose delivery. Investigations considering the patient's curvature using cylindrical or spherical phantoms, as well as more treatment applicators (circular and square) with different bone thicknesses are in progress.

Conflict of Interest

None declared.

Acknowledgements

Photon beam measurements were based on the commissioning of the Gulmay D3225 orthovoltage unit carried out by Drs. M. van Prooijen, A. Beiki, R. Heaton and D. Galbraith in the Princess Margaret Hospital. In addition, authors would like to thank Salmoehe Jelveh for performing the Gafchromic film measurement and Daniel Markel his help in analyzing the measured results. J.C.L.C. would like to thank Ms. Amada Tulk from Gulmay Medical to allow us to share the Monte Carlo input data from Dr. T. Knoos in the Lund University Hospital for verification of the photon beam. This study is supported by the Dean's Fund Grant at the University of Toronto.

REFERENCES

1. McCullough EC. Selection of techniques for orthovoltage radiation therapy. *Int J Radiat Oncol Biol Phys* 1990;18:1237–8.
2. Gao W, Raeside DE. Orthovoltage radiation therapy treatment planning using Monte Carlo simulation: treatment of neuroendocrine carcinoma of the maxillary sinus. *Phys Med Biol* 1997;42:2421.
3. Amdur RJ, Kalbaugh KJ, Ewald LM, et al. Radiation therapy for skin cancer near the eye: kilovoltage X-rays versus electrons. *Int J Radiat Oncol Biol Phys* 1992;23:769–79.
4. Carlsson CA. Differences in reported backscatter factors for low-energy X-rays: a literature study. *Phys Med Biol* 1992;38:521–31.
5. Kawrakow I, Rogers DWO. The EGSnrc code system: Monte Carlo simulation of electron and photon transport. NRCC Report PIPRS-701. Ottawa: National Research Council of Canada; 2000.
6. Kawrakow I. Electron impact ionization cross sections for EGSnrc. *Med Phys* 2002;29:1230.
7. Kawrakow I, Rogers DWO, Walters BR. Large efficiency improvements in BEAMnrc using directional bremsstrahlung splitting. *Med Phys* 2004;31:2883–98.
8. Rogers DWO, Faddegon BA, Ding GX, Ma CM, Wei J, Mackie TR. BEAM: a Monte Carlo code to simulate radiotherapy treatment units. *Med Phys* 1995;22:503–24.
9. Knoos T, Rosenschold P, Wieslander E. Modelling of an orthovoltage X-ray therapy unit with the EGSnrc Monte Carlo package. *J Phys: Conf Series* 2007;74:012009.

10. Ma CM, Coffey CW, Dewerd LA, et al. AAPM protocol for 40–300 kV X-ray beam dosimetry in radiotherapy and radiobiology. *Med Phys* 2001;**28**:868.
11. Ma CM, Reckwerdt P, Holmes M, Rogers DWO, Geiser B. DOSXYZ user manual. NRC Report PIRS 509b; 1995.
12. Toossi MT, Ghorbani M, Mowlavi AA, et al. Air kerma strength characterization of a GZP6 Cobalt-60 brachytherapy source. *Rep Pract Oncol Radiother* 2010;**15**(6):190–4.
13. Mainegra-Hing E, Rogers DWO, Kawrakow I. Calculation of photon energy deposition kernels and electron dose point kernels in water. *Med Phys* 2005;**32**:685–99.
14. Walters BRB, Kawarakow I, Rogers DWO. History by history statistical estimators in the BEAM code system. *Med Phys* 2002;**29**:2745–52.
15. Das IJ. Forward dose perturbation at high atomic number interface in kilovoltage X-ray beams. *Med Phys* 1997;**24**:1781–7.
16. Das IJ, Chopra KL. Backscatter dose perturbation in kilovoltage photon beams at high atomic number interfaces. *Med Phys* 1995;**22**:767–73.
17. ICRU29 Dose specifications for reporting external beam therapy with photons and electrons. ICRU Report No. 29. Bethesda, MD: ICRU; 1978.
18. ICRU50 Prescribing, recording and reporting photon beam therapy. ICRU Report No. 50. Bethesda, MD: ICRU; 1993.
19. Healy BJ, Sylvander S, Nitschke KN. Dose reduction from loss of backscatter in superficial X-ray radiation therapy with Pantak SXT 150 unit. *Australas Phys Eng Sci Med* 2008;**31**:49–55.